Uluslararası İleri Doğa Bilimleri ve Mühendislik Araştırmaları Dergisi
Sayı 8, S. 36-47, 10, 2024

Araştırma Makalesi

IJANSER
https://as-proceeding.com/index.php/ijanser
ISSN:2980-0811

International Journal of Advanced Natural Sciences and Engineering Researches
Volume 8, pp. 36-47, 10, 2024

Research Article

Determination of radiation shielding properties in $BaO–Fe_2O_3–SrO–B_2O_3$ glass systems doped with Bi_2O_3

Selim KAYA[*1]

[1] *Department of Physics Engineering, Faculty of Engineering and Natural Sciences,* Gümüşhane University, Turkey

[*] *selimkaya@gumushane.edu.tr*

(Received: 06 November 2024, Accepted: 16 November 2024)

(3rd International Conference on Contemporary Academic Research ICCAR 2024, 10-11 November 2024)

ATIF/REFERENCE: Kaya, S. (2024). Determination of radiation shielding properties in BaO–Fe2O3–SrO–B2O3 glass systems doped with Bi2O3, *International Journal of Advanced Natural Sciences and Engineering Researches*, 8(10), 36-47.

Abstract – In this study, the effect of Bi_2O_3 incorporation on the radiation shielding performance of $BaO–Fe_2O_3–SrO–B_2O_3$ glass matrices (abbreviated as BBFSB) was systematically evaluated. Using the EGS4 calculation code, the shielding properties were determined and then compared with the data generated by XCOM. An increase in glass density from 3.770 g/cm³ to 5.00 g/cm³ was observed when the Bi_2O_3 concentration was increased. Several key shielding parameters were determined, including the half value layer (HVL), mean free path (MFP), radiation protection efficiency (RPE), fast neutron macroscopic cross-section ΣR (cm^{-1}) and gamma–ray kerma coefficients (κ). The results indicate that increased BiO_3 concentrations significantly improve the material's radiation shielding properties, especially with regard to photon and neutron attenuation, which strengthens the glass system's overall shielding power.

Keywords: Glass Systems, Radiation Protection Efficiency, γ-Kerma Coefficient, EGS4.

I. INTRODUCTION

In many scientific and practical fields, the way materials behave when exposed to gamma-ray radiation is crucial. Applications for gamma photons may be found in imaging, radiation, medical physics, space technology, and more. Radiation physicists and nuclear engineers are motivated to investigate more appropriate radiation shielding solutions by the growing prevalence of application in various sectors. Because of its penetration, gamma-ray photons are widely used in many different sectors, and their interaction with matter is a focus of study and development. Knowing how materials react to gamma-ray radiation is essential for designing shields, detection systems, and reducing background noise in high-energy particle physics investigations.

For practical use in these fields, research endeavors concentrate on creating materials that not only efficiently attenuate gamma-ray radiation but also satisfy requirements like weight efficiency, durability, and cost-effectiveness. [1-2]. It is well known that adding heavy metals to glass composition greatly improves its radiation shielding capabilities.

An essential metric for comprehending how radiation and materials interact is the mass attenuation coefficient, or MAC. This coefficient, which has applications in business, health, and research, quantifies how well a substance lowers radiation intensity as it travels through. For example, in medical imaging, different radiation types, including CT scans and X-rays, have different attenuation coefficients in the human body's tissues. Accurate understanding of these factors is essential since they have a direct impact

on the diagnostic quality and clarity of medical pictures, allowing for a more realistic depiction of interior structures and any anomalies. By taking these factors into account while optimizing imaging methods, detailed and therapeutically valuable pictures are guaranteed.

Understanding the MAC for different shielding materials is essential for radiation protection. This knowledge is essential for creating and putting into place efficient barriers to lower radiation exposure in places where radiation is a concern, such as nuclear power plants, hospitals, and industrial settings. These coefficients are used by engineers and safety specialists to choose materials and create structures that effectively reduce radiation, improving safety procedures.

Additionally, the MAC assists personnel in selecting appropriate shielding materials and correctly interpreting radiography data in industrial radiography, where radiation is used to check materials for flaws or to perform quality control. Accurate material analysis and dependable flaw identification are ensured by knowledge of the attenuation characteristics of various substances.

All things considered, researching the MAC gives researchers vital information on the make-up, structure, and physical characteristics of materials. This knowledge promotes technological, safety engineering, medical imaging, and scientific research improvements, highlighting the coefficient's crucial importance in a variety of fields.

Understanding the behavior of samples when exposed to gamma-ray radiation is crucial for developing materials that are more resistant to such radiation. Parameters like the mass attenuation coefficient (MAC), radiation protection efficiency (RPE), and gamma-ray kerma coefficient (kγ) are vital in designing materials that can withstand high-energy particle physics experiments [3].

The Radiation Protection Efficiency (RPE) quantifies a material's effectiveness in shielding against radiation exposure. Fast neutron removal cross sections represents the time per unit path length during which a neutron is exposed to a specific type of transmission (such as absorption or scattering) in a given material. Additionally, the Gamma-ray Kerma Coefficient (kγ) assesses the energy transferred to the material by gamma-ray photons through various interaction.

The XCOM software was developed by Berger and Hubbell as a tool for calculating the mass attenuation coefficients and photon cross sections for elements, compounds, and mixtures over a wide range of energies, from 1 keV to 100 GeV [4]. To make the software more accessible and user-friendly, Gerward et al. developed a modified version of XCOM known as WinXCOM [5]. Mass attenuation coefficients and other factors crucial to comprehending gamma-ray interactions were computed using Monte Carlo techniques, which simulate the behavior of gamma rays as they travel through materials. [6-11].

In this study, the mass attenuation coefficients of glasses doped with Bi2O3 were theoretically Monte Carlo EGS4 and winXCOM calculated energies from 59,5 to 1332 keV. The theoretically calculated mass attenuation coefficient (MAC) values from XCOM and EGS4 were employed to derive several shielding parameters, including the mean free path (MFP), half-value layer (HVL), radiation protection efficiency (RPE), fast neutron macroscopic cross-section ΣR (cm−1) and gamma kerma coefficients (kγ).

II. MATERIALS AND METHOD

Monte Carlo Simulation

In the present investigation, EGS4 (Electron Gamma Showers) Nelson and Hirayama was utilized to calculate kerma coefficients and gamma attenuation parameters [12]. To model the HPGe detector response, Monte Carlo simulations were performed using the EGS4. Using a certified random number generator is essential for MC calculations since random number production is crucial. The EGS4 code was implemented using a RANLUX random number generator, which has been demonstrated to generate a longer sequence and a comparatively superior distribution [13]. 10,010 energy bins with a width of 0.3 keV each were created from the efficiency for the model run using EGS4. After dividing the computed

area into 241 cells, the form is rotated 360 degrees on the -axis shown in Fig. 1 to produce a cylindrical geometry. Assumedly, Fig. 1 depicts a sequence of cylindrical circular projectiles, each having a plane denoted by P1, P2, …., P20, and a radius denoted by R1, R2, …, R11. For the point radioactive source, a section of code was written such that all photons were emitted along the z-axis, producing a beam of collimated photons. [7,8,14].

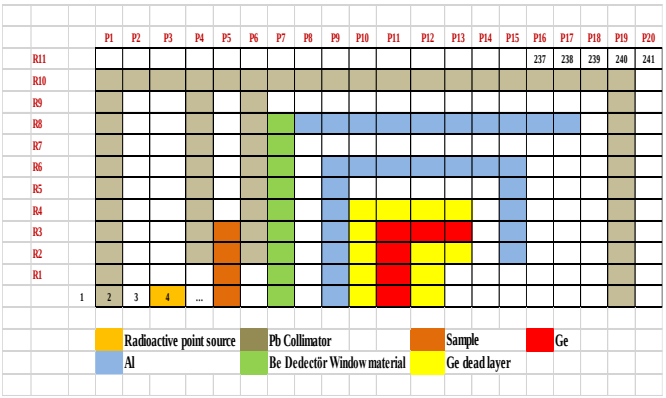

Fig. 1. Detector model for Monte Carlo (ESG4 code) calculations.

Gamma attenuation parameters

In this study, the mass attenuation coefficients (MAC) parameters of samples were determined as follows:

The attenuation of gamma rays in a material can be described using the Beer-Lambert law, which states:

$$I = I_0 e^{-\mu x} \qquad (1)$$

where I is the intensity of the gamma-ray beam after it has passed through a thickness x of the material, I_0 is the initial intensity of the beam and μ (cm^{-1}) is the linear attenuation coefficient of the material for the specific energy of the gamma rays being considered.

While the linear attenuation coefficient (μ) is commonly used to describe how strongly a material absorbs gamma rays, it has the disadvantage of depending on the density of the material. Therefore, it is often more useful to use the density-independent mass attenuation coefficient (μ/ρ), which is expressed in units of cm^2/g.

The density-independent mass attenuation coefficient can be calculated using the following formula μ/ρ (cm^2/g):

$$I = I_0 e^{-(\mu/\rho)\rho x} = I_0 e^{-(\mu/\rho)d} \qquad (2)$$

According to the Beer-Lambert law equation, the thickness "d" is expressed in unit area mass of the material (g/cm^2). When a sample contains more than one metal, the mass attenuation coefficient (μ/ρ) of the sample can be calculated using the mixture rule formula, which is given as:

$$\mu/\rho = \sum_i w_i (\mu/\rho)_i \qquad (3)$$

where w_i is the weight fraction of the ith component in the sample and $(\mu/\rho)_i$ is the density-independent mass attenuation coefficient of the ith component [15].

The weight fraction (wi) of a chemical component i in a mixture can be calculated using the following relation:

$$w_i = \frac{a_i A_i}{\sum a_i A_i} \quad (4)$$

where a_i is the number of formula units, *Ai* is the atomic weight of the ith element, and the summation is taken over all components in the mixture.

Mass attenuation coefficients (μ ρ/) of the samples under study are computed by Monte Carlo-EGS4 simulation code and compared to WinXCOM results in the energy range 0.0595–1.332 MeV. The theoretical mass attenuation coefficients (μ/ρ) of samples were determined using WinXCom software [5,7,16,17].

Half value layer (HVL) of the materials is the thickness that reduced the half of the radiation entering it [18]: The HVL can be calculated using the following equation

$$HVL = ln2/\mu \quad (6)$$

The mean free path (MFP) is a measure of the average distance a particle or photon can travel in a material before it interacts with the material in some way, such as absorption, scattering, or transmission. In general, the MFP is the inverse of the linear attenuation coefficient (μ) of a material, which describes how much radiation is absorbed or scattered per unit length of the material. The mean free path (MFP) were calculated using μ values as follows [19]:

$$MFP = 1/\mu \quad (8)$$

where, μ is the linear attenuation coefficient, whose unit of measurement is cm^{-1}.

The radiation protection efficiency (RPE) parameter of sampless was investigated. The efficiency (RPE) in terms from incoming and transmitted photon densities is given equation below [20]:

$$RPE = \left(1 - \frac{I}{I_0}\right) * 100 \quad (9)$$

Kerma coefficient ($Gy.cm^2$/photon) for uncharged particles can be calculated using the mass attenuation coefficient and partial interaction probabilities. It is given by the equation:

$$K = k\phi\left[\frac{\mu_{tr}}{\rho}\right] \quad (10)$$

where K is uncharged radiation of energy E, $k\phi$ is the kerma coefficient and μ_{tr}/ρ is the mass energy-transfer coefficient of the substance [21]: (11)

Methods for finding the photon kerma coefficients of samples have been given in previous studies [7,10,22,23]:

A key metric in nuclear reactor analysis and neutron transport theory is the fast neutron macroscopic cross-section ΣR (cm−1), which captures the interaction probability per unit distance traveled by fast neutrons in a material medium. The following relationship is used to get the ΣR value for neutron shielding materials.

$$\Sigma_R / \rho = \sum_i w_i (\Sigma_R/\rho)_i \quad (11)$$

and

$$\Sigma_R = \sum_i \rho_i (\Sigma_R/\rho)_i \quad (12)$$

where the partial density of the ith element is represented by ρi (g/cm^3) and the fast neutron removal cross section by ΣR/ρ (cm^2/g) [18,24,26]: The following formula can be used to determine the partial density of the i-th element, represented as (ρi):

$$\rho_i = \rho \times w_i \quad (13)$$

Here, wi stands for the weight fraction of the ith element, and ρ for the sample's density (g/cm^3). [18]:

III. RESULTS AND DISCUSSION

Using x values of 0, 5, 10, 15, and 20 mol%, the current study assessed the impact of different Bi_2O_3 concentrations on the radiation shielding efficacy of (x)Bi_2O_3– (20−x)BaO – 60B_2O_3 – 0.3Fe_2O_3 – 19.7 SrO glass composition. [27,28]:

Chemical composition of BBFSB glasses system doped with Bi_2O_3 (% weight percentage) is given Table 1. Calculated EGS4 and XCOM mass attenuation coefficients μ/ρ (cm^2 g^{-1}), samples at different 11 energies from 59.54 to 1332 keV have been given in Table 2. Theoretical (K_T) and simulation (K_{EGS4}) kerma coefficients for the samples have been given in Table 3.. The variation of the mass attenuation coefficients with the energy for samples is given Fig 2. BaO–Fe_2O_3–SrO–B_2O_3 glass matrices doped with Bi_2O_3 change graph of HVL and MFP values versus photon energy. Variation of energy with half value layer (HVL) and mean free path (MFP) for given samples was plotted in the 1 keV–100 MeV energy range and shown in Fig 3 and 4, respectively. As photon energy increases, it can be observed from these figures that the Half Value Layer (HVL) and Mean Free Path (MFP) values for the samples under investigation both rise.

Fig. 5 shows changes of RPE with photon energy for investigated samples. In figure 5, it is seen that the RPE values decrease as the photon energy increases.

Furthermore, the different samples ΣR were computed and shown in Fig 6. As seen in Figure 6, BFSB-5 has the largest ΣR (cm^{-1}) value compared to other samples. As a result of its higher density in comparison to the other samples, the BFSB-5 glass sample shows an enhanced total interaction cross-section (ΣR). It is therefore the most effective material for absorbing neutrons and offers superior defense against gamma radiation.

The graph of change of gamma kerma coefficients for samples is shown in Fig. 7. The relative dominance of many photon interaction mechanisms, such as the photoelectric effect, Compton scattering, and pair production, determines the properties of the kerma coefficient curves vs gamma-ray energy. The photon energy and the atomic number of the substance absorbed determine the relative contributions of each of these interaction mechanisms. In the intermediate energy range, the kerma coefficient decreases as photon energy increases because Compton scattering and pair production become more significant in relation to the photoelectric interaction.

Table 1. Chemical composition of BBFSB glasses system doped with Bi_2O_3 (% weight percentage)

BBFSB glasses system doped with Bi_2O_3	Density ρ (g/cm3)	B	O	Fe	Sr	Ba	Bi
BBFSB-1	3.770	13.90	37.80	0.360	18.49	29.45	0.00
BBFSB-2	3.940	11.91	33.86	0.300	15.84	18.90	19.18
BBFSB-3	4.183	10.41	30.90	0.270	13.85	11.02	33.55
BBFSB-4	4.617	9.250	28.59	0.240	12.31	4.900	44.71
BBFSB-5	5.000	8.325	26.75	0.210	11.08	0.00	53.63

Table 2. Calculated (EGS4) and Theoretical (XCOM) values of mass attenuation coefficients μ/ρ (cm^2/g)

Mass attenuation coefficients μ/ρ (cm^2/g)										
Energy (keV)	**Sample-1**		**Sample-2**		**Sample-3**		**Sample-4**		**Sample-5**	
	XCOM	EGS4	XCOM	EGS4	XCOM	EGS4	XCOM	EGS4	XCOM	EGS4
59.54	3.268	3.269	3.279	3.274	3.287	3.278	3.294	3.296	3.299	3.295
122	0.556	0.552	1.064	1.061	1.444	1.414	1.740	1.744	1.976	1.979
200	0.220	0.221	0.363	0.360	0,470	0.467	0.553	0.551	0.620	0.621
300	0.133	0.133	0.184	0.181	0,221	0.225	0.251	0.249	0,274	0.271
383	0.108	0.106	0.135	0.138	0,155	0.160	0.171	0.168	0,184	0.183
511	0.088	0.085	0.101	0.103	0,111	0.114	0.119	0.121	0,125	0.121
662	0.075	0.079	0.082	0.084	0,088	0.084	0.092	0.088	0,095	0.092
800	0.068	0.071	0.072	0.073	0,076	0.073	0.078	0.079	0,080	0.085
1000	0.060	0.062	0.063	0.064	0,064	0.062	0.066	0.066	0,067	0.071
1274	0.053	0.055	0.054	0.055	0,055	0.056	0.056	0.059	0,057	0.058
1332	0.052	0.054	0.053	0.054	0,054	0.054	0.054	0.057	0,055	0.057

Table 3. Calculated (EGS4) and Theoretical (XCOM) values of kerma coefficients *k* (in pGy.cm2/photon)

Kerma coefficients *k* (in pGy.cm2/photon)										
Energy (keV)	**Sample-1**		**Sample-2**		**Sample-3**		**Sample-4**		**Sample-5**	
	XCOM	EGS4	XCOM	EGS4	XCOM	EGS4	XCOM	EGS4	XCOM	EGS4
59.54	28.854	28.866	28.400	28.359	28.059	28.972	27.795	27.818	27.583	27.555
122	8.184	8.122	17.773	17.724	24.956	24.438	30.538	30.613	35.000	35.061
200	3.868	3.889	8.248	8.192	11.528	11.464	14.077	14.021	16.115	16.142
300	2.738	3.077	5.039	5.295	6.762	7.214	8.102	8.380	9.172	9.398
383	2.619	3.000	4.203	4.734	5.389	5.975	6.311	6.592	7.048	7.416
511	2.833	3.533	3.873	4.773	4.652	5.588	5.258	6.132	5.742	6.328
662	3.270	4.162	3.998	4.811	4.543	5.004	4.967	5.396	5.306	5.780
800	3.711	3.645	4.278	4.105	4.702	4.348	5.032	4.857	5.296	5.408
1000	4.347	4.788	4.771	5.211	5.088	5.150	5.334	5.656	5.531	6.162
1274	5.147	5.450	5.456	5.582	5.691	5.829	5.867	6.299	6.011	6.211
1332	5.334	5.561	5.629	5.728	5.849	5.848	6.021	6.266	6.158	6.335

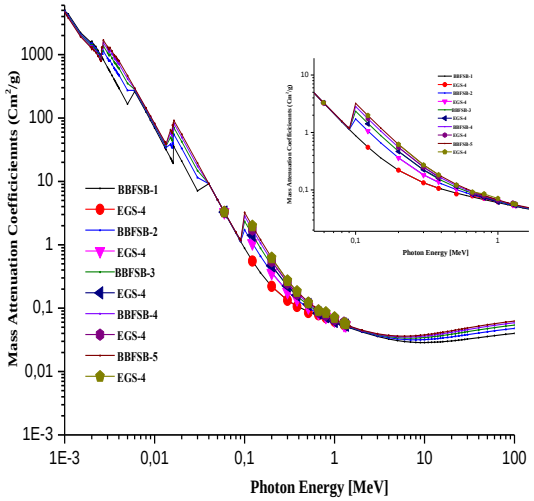

Fig. 2. The variation of the mass attenuation coefficients with the energy for samples.

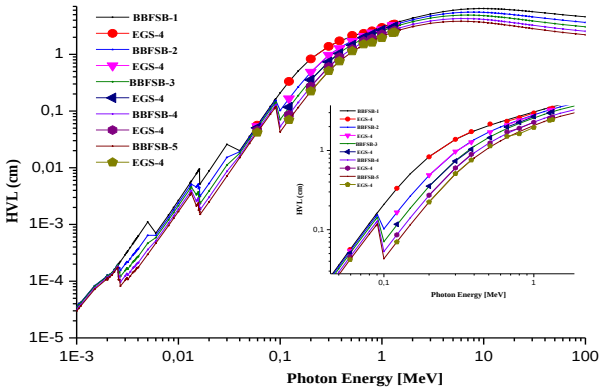

Fig. 3. The variation of the half value layer (HVL) with the energy for glasses doped with Bi_2O_3

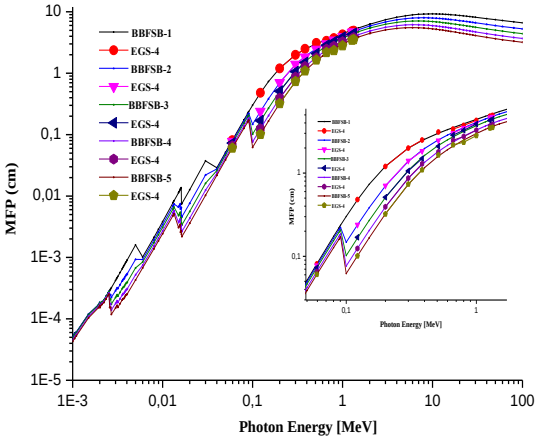

Fig. 4. The variation of the mean free path (MFP) with the energy for glasses doped with Bi_2O_3

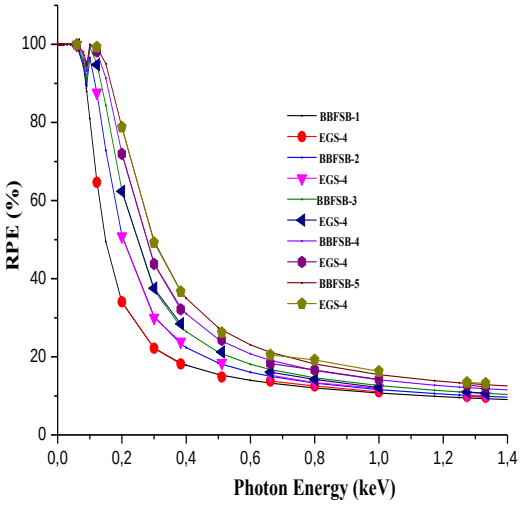

Fig. 5. The variation of radiation protection efficiency (RPE) of samples versus the photon energy

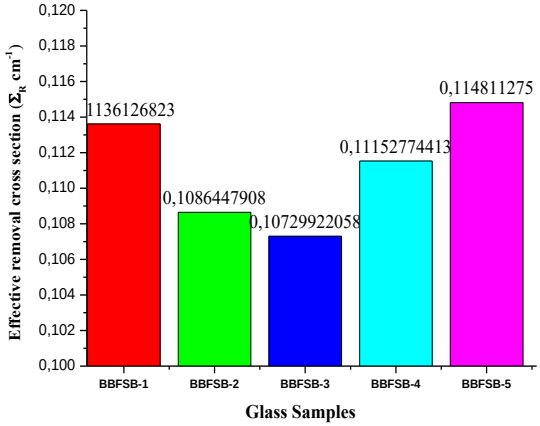

Fig. 6. Fast neutron macroscopic cross-section ΣR (cm^{-1}) of the given glass samples

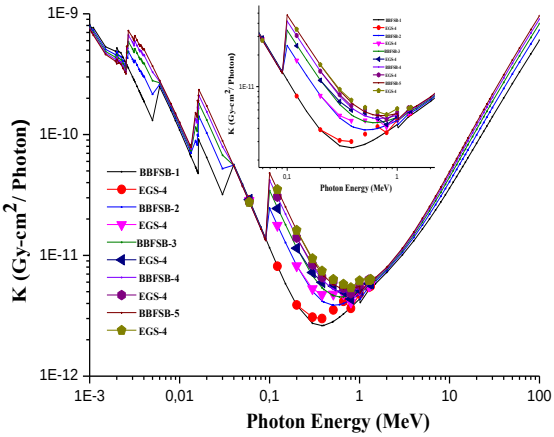

Fig. 7. The gamma kerma coefficients of samples as a function of photon energy

IV. CONCLUSION

This study seeks to investigate the influence of stoichiometric modifications in glasses doped with Bi_2O_3 on radiation shielding parameters at gamma-ray energies from 59,5 to 1332 keV. Mass attenuation coefficients (μ/ρ) for glasses doped with Bi_2O_3 were investigated theoretically (WinXcom and EGS4). It was determined some shielding parameters such as mean free path (MFP), half value layer (HVL), radiation protection efficiency (RPE), fast neutron macroscopic cross-section ΣR (cm−1) and gamma–ray kerma coefficients (kγ).

As the density of Bi_2O_3 doped glasses increases, a significant decrease in mass attenuation coefficients is observed, especially up to the first 500 keV. A decrease in the mean free path (MFP) in the half-value layer (HVL) at a fixed energy level for Bi_2O_3 doped glass samples resulted in a significant increase in radiation shielding efficiency (RPE) and gamma-ray kerma coefficients.

For the same energy values, it was observed that as the Bi_2O_3 contribution increased, the Half value layer (HVL), mean free path (MFP), values of the samples decreased, radiation shielding efficiency (RPE) and gamma-ray kerma coefficients (kγ) increased. In many different domains, it is crucial to research how materials react to radiation, particularly gamma rays and neutrons. In nuclear power plants, medical imaging, space exploration, and even common applications where radiation exposure needs to be minimized, effective shielding materials are crucial. Researchers can create better shielding materials by knowing how different materials react to radiation and attenuate it. This entails not only enhancing shielding capabilities but also using materials effectively to provide shielding solutions that are lighter, more resilient, and more affordable. Calculating radiation protection parameters for glass samples is of paramount importance in enhancing safety protocols, optimizing material properties, and contributing to the advancement of radiation shielding technologies. This study facilitates the development of glass systems that not only demonstrate efficacy and safety but also exhibit innovative characteristics, specifically tailored for applications in environments where radiation exposure poses a considerable risk.

REFERENCES

[1] Ersundu, A. E., Büyükyıldız, M., Ersundu, M. Ç., Şakar, E., & Kurudirek, M. J. P. N. E. (2018). The heavy metal oxide glasses within the WO3-MoO3-TeO2 system to investigate the shielding properties of radiation applications. *Progress in Nuclear Energy*, *104*, 280-287.

[2] Kaewkhao, J., & Limsuwan, P. (2010). Mass attenuation coefficients and effective atomic numbers in phosphate glass containing Bi2O3, PbO and BaO at 662 keV. Nuclear Instruments and Methods in Physics Research Section A: Accelerators, Spectrometers, Detectors and Associated Equipment, 619(1-3), 295-297.

[3] Baltaş, H., Çelik, Ş., Çevik, U., Yanmaz, E., 2007. Measurement of mass attenuation coefficients and effective atomic numbers for MgB2 superconductor using X-ray energies. Radiat. Meas. 42, 55–60.

[4] Berger, M. J., & Hubbell, J. H. (1999). XCOM: Photon cross-sections on a personnel computer (version 1.2). *NBSIR85-3597, National Bureau of Standarts, Gaithersburg, MD, USA, for version*, *3*.

[5] Gerward, L., Guilbert, N., Jensen, K.B., Levring, H., 2001. X-ray absorption in matter. Reengineering XCOM. Radiat. Phys. Chem. 60, 23–24.

[6] Tekin, H.O., Singh, V.P., Manici, T., 2017. Effects of micro-sized and nano-sized WO 3 on mass attenauation coefficients of concrete by using MCNPX code. Appl. Radiat. Isot. 121, 122–125.

[7] Baltas, H. (2020). Evaluation of gamma attenuation parameters and kerma coefficients of YBaCuO and BiPbSrCaCuO superconductors using EGS4 code. Radiation Physics and Chemistry, 166, 108517.

[8] Kaya, S., Çelik, N., and Bayram, T. (2022). Effect of front, lateral and back dead layer thicknesses of a HPGe detector on full energy peak efficiency. Nuclear Instruments and Methods in Physics Research Section A: Accelerators, Spectrometers, Detectors and Associated Equipment, 1029, 166401.

[9] El-Khayatt, A.M., Vega-Carrillo, H.R., 2015. Photon and neutron kerma coefficients for polymer gel dosimeters. Nucl. Instruments Methods Phys. Res. Sect. A Accel. Spectrometers, Detect. Assoc. Equip. 792, 6–10.

[10] El-Khayatt, A.M., 2017. Semi-empirical determination of gamma-ray kerma coefficients for materials of shielding and dosimetry from mass attenuation coefficients. Prog. Nucl. Energy 98, 277–284.

[11] Kaya, S., Çelik, N., Gök, A., & Çevik, U. (2023). Effect of detector crystal size on Compton suppression factors. Radiation Effects and Defects in Solids, 178(11-12), 1449-1462.

[12] Nelson, W.R., Rogers, D.W.O., Hirayama, H., 1985. The EGS4 code system.

[13] *Gasparro, J., Hult, M., Johnston, P.N., Tagziria, H., 2008. Monte Carlo modelling of germanium crystals that are tilted and have rounded front edges. Nucl. Instruments Methods Phys. Res. Sect. A Accel. Spectrometers, Detect. Assoc. Equip. 594, 196–201*

[14] Kaya, S. (2023). Calculation of the effects of silver (Ag) dopant on radiation shielding efficiency of BiPbSrCaCuO superconductor ceramics using EGS4 code. *Applied Sciences*, *13*(14), 8358.

[15] Kumar, A., Gaikwad, D.K., Obaid, S.S., Tekin, H.O., Agar, O., Sayyed, M.I., 2020. Experimental studies and Monte Carlo simulations on gamma ray shielding competence of (30+ x) PbO10WO3 10Na2O− 10MgO–(40-x) B2O3 glasses. Prog. Nucl. Energy 119, 103047

[16] Celik, N., Cevik, U., 2010. Monte Carlo determination of water concentration effect on gamma-ray detection efficiency in soil samples. Appl. Radiat. Isot. 68, 1150–1153

[17] *Gerward, L., Guilbert, N., Jensen, K.B., Leving, H., 2004. WinXCom–a program for calculating X-ray attenuation coefficients. Radiat. Phys. Chem. 71, 653–654*

[18] Tekin, H.O., Altunsoy, E.E., Kavaz, E., Sayyed, M.I., Agar, O., Kamislioglu, M., 2019. Photon and neutron shielding performance of boron phosphate glasses for diagnostic radiology facilities. Results Phys. 12, 1457–1464.

[19] Gaikwad, D.K., Sayyed, M.I., Botewad, S.N., Obaid, S.S., Khattari, Z.Y., Gawai, U.P., Afaneh, F., Shirshat, M.D., Pawar, P.P., 2019. Physical, structural, optical investigation and shielding featuresof tungsten bismuth tellurite-based glasses. J. Non. Cryst. Solids 503, 158–168.

[20] Sayyed, M. I., Akman, F., Kumar, A., & Kaçal, M. R. (2018). Evaluation of radioprotection properties of some selected ceramic samples.Results in Physics, 11, 1100-1104.

[21] Thomas, D.J., 2012. ICRU report 85: fundamental quantities and units for ionizing radiation.

[22] Attix, F.H., 2008. Introduction to Radiological Physics and Radiation Domisetry, John Wiley & Sons, U.S.A.

[23] Abdel-Rahman, W., Podgorsak, E.B., 2010. Energy transfer and energy absorption in photon interactions with matter revisited: A step-by-step illustrated approach. Radiat. Phys. Chem.

[24] El-Agawany, F. I., Kavaz, E., Perişanoğlu, U., Al-Buriahi, M., & Rammah, Y. S. (2019). Sm 2 O 3 effects on mass stopping power/projected range and nuclear shielding characteristics of TeO 2–ZnO glass systems. Applied Physics A, 125, 1-12.

[25] Yılmaz, E., Baltas, H., Kırıs, E., Ustabas, I., Cevik, U., El-Khayatt, A.M., 2011. Gamma ray and neutron shielding properties of some concrete materials. Ann. Nucl. Energy 38, 2204–2212.

[26] Sirin, M. (2020). The effect of titanium (Ti) additive on radiation shielding efficiency of Al25Zn alloy. Progress in nuclear energy, 128, 103470.

[27] Kheswa, B. V., & Majola, S. N. (2024). Investigation of the effect of bismuth-oxide on the X-ray and neutron shielding efficacy of the new ceramic system Bi_2O_3–BaO–Fe_2O_3–SrO–B_2O_3. Journal of Theoretical and Applied Physics, 18(5), 1-9.

[28] Babeer, A. M., Amin, H. Y., Sayyed, M. I., Mahmoud, A. E. R., Abdo, M. A., Ellakwa, T. E., & Sadeq, M. S. (2024). Impact of mixed heavy metal cations (Ba and Bi) on the structure, optical and ionizing radiation shielding parameters of Bi_2O_3–BaO–Fe_2O_3–SrO–B_2O_3 glass matrix. Ceramics International, 50(11), 19245-19258.